

Supplementary Materials

Hybrid Metamaterials for Decoupled Electromagnetic-Acoustic Wave Manipulation: Achieving Four Negative Constitutive Parameters

Zhaolun Yu,^{a,b} Tian Gan,^a Xiaole Wang,^{a,*} Chunyu Zhao,^a Zhenyu Huang,^a and Xudong Luo^{b,*}

^a. *School of Automation and Intelligent Sensing, School of Electronic Information and Electrical Engineering, Shanghai Jiao Tong University, Shanghai 200240, China*

^b. *School of Physics and Astronomy, Key Laboratory of Artificial Structures and Quantum Control (Ministry of Education), and National Demonstration Centre for Experimental Physics Education, Shanghai Jiao Tong University, Shanghai 200240, China.*

1. Structural parameters of a unit cell	2
2. Retrieval procedure of electromagnetic constitutive parameters of an electromagnetic functional module.....	3
3. Retrieval procedure of acoustic constitutive parameters of an acoustic functional module	5
4. Numerical models based on the finite element method.....	6
5. Effective electromagnetic and acoustic refractive indices of the metamaterial.....	8
6. Experimental setup for retrieving acoustic parameters	9
7. Comparison between measured and simulated acoustic constitutive parameters	9
8. Constituent material parameters for the hybrid metamaterial samples.....	10

1. Structural parameters of a unit cell

The unit cell consists of two 3D-printed components: a base and a lid. The base includes grooves and columns, and the lid is a simple frame with several square through-holes. The printed circuit boards (PCBs), each 0.8mm in thickness, pass through the holes in the lid, securing the PCBs in place. The unit cell incorporates four types of PCBs, each printed with a two-dimensional periodic array of split-ring resonators and thin strips on the back. Each array measures $4 \text{ mm} \times 4 \text{ mm}$. The first type of PCB consists of a 1×15 array, resulting in dimensions of $4 \text{ mm (length)} \times 60 \text{ mm (height)}$. The second type features a 4×15 array, measuring $16 \text{ mm (length)} \times 60 \text{ mm (height)}$. The third type has a 5×15 array, with dimensions of $20 \text{ mm (length)} \times 60 \text{ mm (height)}$. The fourth type includes a 10×15 array, measuring $40 \text{ mm (length)} \times 60 \text{ mm (height)}$. A photo of all the components is shown in Fig. S1.

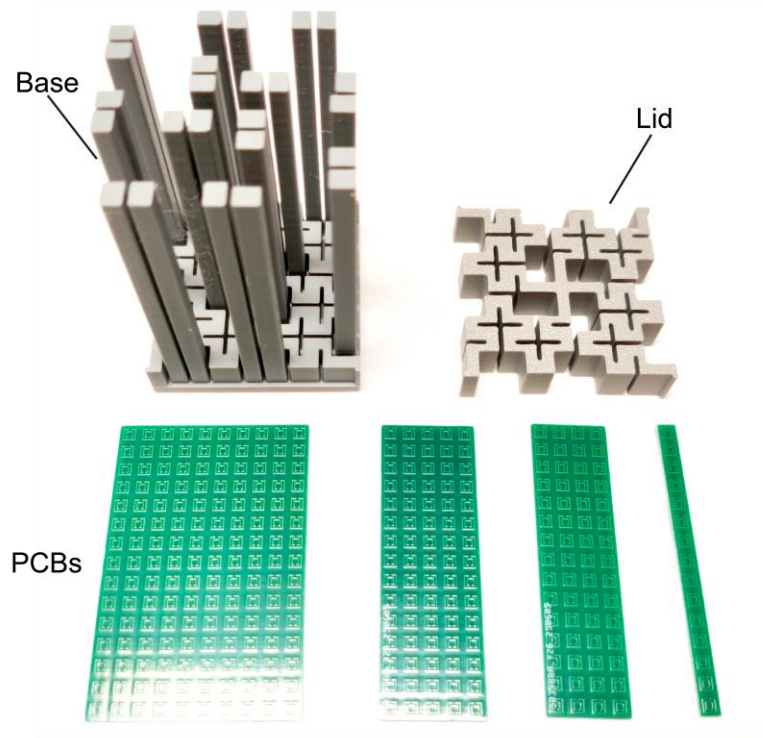


FIG. S1 Photo of the basic constituent components in a unit cell

As marked in Fig.1 (c) and (d) in the main text, the geometric parameters of the electromagnetic functional module are as follows: $l_{e1} = 4.00 \text{ mm}$, $l_{e2} = 0.30 \text{ mm}$, $l_{e3} = 0.30 \text{ mm}$, $w_{e1} = 0.25 \text{ mm}$, $w_{e2} = 0.46 \text{ mm}$, $w_{e3} = 0.46 \text{ mm}$, $w_{e2} = 4.00 \text{ mm}$. As marked in Fig.1 (e) in the main text, the geometric parameters of the acoustic functional module are as follows: $l_{a1} =$

45.40 mm , $l_{a2} = 4.50$ mm , $l_{a3} = 2.65$ mm , $w_{a1} = 0.87$ mm , $w_{a2} = 3.13$ mm , $w_{a3} = 20.50$ mm, $w_{a4} = 16.50$ mm, $w_{a5} = 40.50$ mm. The electromagnetic functional module has a dimension of 4 mm, which is less than one-seventh of the X-band center wavelength (30 mm), while the acoustic functional module has a dimension of 45.40 mm, which is less than one-sixth of the wavelength of acoustic waves at 1200 Hz (285 mm). This allows for homogenization in both electromagnetic and acoustic domains.

2. Retrieval procedure of electromagnetic constitutive parameters of an electromagnetic functional module

The effective electromagnetic constitutive parameters of an electromagnetic functional module are extracted using an S-parameter inversion procedure. Let a_1 and a_2 be the normalized amplitudes of the incident electromagnetic waves at ports 1 and 2, and b_1 and b_2 the corresponding amplitudes of outgoing electromagnetic waves. These quantities satisfy

$$\begin{pmatrix} b_1 \\ b_2 \end{pmatrix} = \begin{pmatrix} S_{11} & S_{12} \\ S_{21} & S_{22} \end{pmatrix} \begin{pmatrix} a_1 \\ a_2 \end{pmatrix}, \quad (S1)$$

where S_{11} , S_{12} , S_{21} and S_{22} are the elements of the scattering matrix. Consider a unit-amplitude electromagnetic plane wave, polarized along the z -axis and described by

$$\mathbf{E}_{iz} = e^{-jk_{e0}z + j\omega t}, \quad (S2)$$

incident at $z = -z_s$ (port 1). The wave propagates through the metamaterial with an effective length d_e , and is received at $z = z_s$ (port 2). $k_{e0} = \omega/c_{e0}$ is the free-space electromagnetic wavenumber, where ω is the angular frequency and c_{e0} the phase velocity of electromagnetic waves in the air. For brevity, the common time-harmonic factor $e^{j\omega t}$ can be omitted. Thus, the electric and magnetic fields at port 1 and at the two interfaces of the metamaterial can be written as

$$\mathbf{E}_i = e^{-jk_{e0}(z+z_s)}, \mathbf{H}_i = -\frac{k_{e0}}{\omega\mu_0} [e^{-jk_{e0}(z+z_s)}], \quad (S3)$$

$$\mathbf{E}_r = Ae^{jk_{e0}z}, \mathbf{H}_r = -\frac{k_{e0}}{\omega\mu_0} [-Ae^{jk_{e0}z}], \quad (S4)$$

$$\mathbf{E}_t = Ce^{-jk_e z}, \mathbf{H}_t = -\frac{k_e}{\omega\mu_0\mu_{\text{eff}}} [Ce^{-jk_e z}], \quad (S5)$$

$$\mathbf{E}'_r = Xe^{jk_e(z-d_e)}, \mathbf{H}'_r = -\frac{k_e}{\omega\mu_0\mu_{\text{eff}}} [-Xe^{jk_e(z-d_e)}], \quad (S6)$$

$$\mathbf{E}'_t = Ye^{-jk_{e0}(z-d_e)}, \mathbf{H}'_t = -\frac{k_{e0}}{\omega\mu_0} [Ye^{-jk_{e0}(z-d_e)}], \quad (S7)$$

where \mathbf{E}_i and \mathbf{H}_i denote the amplitudes of the incident electric and magnetic fields. At the front

interface of the metamaterial, the reflected fields are \mathbf{E}_r and \mathbf{H}_r , and the transmitted fields are \mathbf{E}_t and \mathbf{H}_t . At the rear interface, the reflected fields become \mathbf{E}'_r and \mathbf{H}'_r , with the transmitted fields \mathbf{E}'_t and \mathbf{H}'_t . The coefficients A and X specify the reflection amplitudes, while C and Y specify the transmission amplitudes. The electromagnetic wavenumber in the metamaterial is given by $k_e = \omega/c_e$, where c_e is the phase velocity inside the metamaterial. The effective refractive index is $n_e = c_{e0}/c_e$ with c_{e0} the phase velocity in the free space of air.

Since the electric and magnetic fields remain continuous at both interfaces of the metamaterial, the following relations hold:

$$\mathbf{E}_i|_{z=0} + \mathbf{E}_r|_{z=0} = \mathbf{E}_t|_{z=0} + \mathbf{E}'_r|_{z=0} \Rightarrow e^{-jk_{e0}z_s} + A = C + Xe^{-jk_e d_e}, \quad (\text{S8})$$

$$\mathbf{H}_i|_{z=0} + \mathbf{H}_r|_{z=0} = \mathbf{H}_t|_{z=0} + \mathbf{H}'_r|_{z=0} \Rightarrow -\frac{k_{e0}}{\omega\mu_0}(e^{-jk_{e0}z_s} - A) = -\frac{k_e}{\omega\mu_0\mu_{\text{eff}}}(C - Xe^{-jk_e d_e}), \quad (\text{S9})$$

$$\mathbf{E}_t|_{z=d_e} + \mathbf{E}'_r|_{z=d_e} = \mathbf{E}'_t|_{z=d_e} \Rightarrow Ce^{-jk_e d_e} + X = Y, \quad (\text{S10})$$

$$\mathbf{H}_t|_{z=d_e} + \mathbf{H}'_r|_{z=d_e} = \mathbf{H}'_t|_{z=d_e} \Rightarrow -\frac{k_e}{\omega\mu_0\mu_{\text{eff}}}(Ce^{-jk_e d_e} - X) = -\frac{k_{e0}}{\omega\mu_0}Y. \quad (\text{S11})$$

Accordingly, A and Y can be computed by

$$A = \frac{r(1 - e^{-j2n_e k_{e0} d_e})}{1 - r^2 e^{-j2n_e k_{e0} d_e}} e^{-jk_{e0} z_s}, \quad (\text{S12})$$

$$Y = \frac{(1 - r^2)e^{-jn_e k_{e0} d_e}}{1 - r^2 e^{-j2n_e k_{e0} d_e}} e^{-jk_{e0} z_s}. \quad (\text{S13})$$

The reflection coefficient r can be obtained by

$$r = \frac{Z_e - 1}{Z_e + 1}, \quad (\text{S14})$$

where Z_e is the characteristic impedance of the metamaterial. Subsequently, the S-parameters S_{11} and S_{21} take the form:

$$S_{11} = \frac{\mathbf{E}_r|_{z=-z_s}}{\mathbf{E}_i|_{z=-z_s}} = Ae^{-jk_{e0} z_s} = \frac{r(1 - e^{-j2n_e k_{e0} d_e})}{1 - r^2 e^{-j2n_e k_{e0} d_e}} e^{-j2k_{e0} z_s}, \quad (\text{S15})$$

$$S_{21} = \frac{\mathbf{E}'_t|_{z=z_s}}{\mathbf{E}_i|_{z=-z_s}} = Ye^{-jk_{e0}(z_s - d_e)} = \frac{(1 - r^2)e^{-jn_e k_{e0} d_e}}{1 - r^2 e^{-j2n_e k_{e0} d_e}} e^{-jk_{e0}(2z_s - d_e)}. \quad (\text{S16})$$

Z_e and n_e can be written as

$$Z_e = \pm \sqrt{\frac{(1 + S_{11})^2 - S_{21}^2}{(1 - S_{11})^2 - S_{21}^2}}, \quad (\text{S17})$$

$$n_e = \frac{1}{k_{e0} d_e} \{ \text{Im}[\ln(e^{jn_e k_{e0} d_e})] + 2m\pi - j\text{Re}[\ln(e^{jn_e k_{e0} d_e})] \}. \quad (\text{S18})$$

Here, m is the integer that indexes the branch of the real part of n_e . Since the metamaterial is passive, both the real part of Z_e and the imaginary part of n_e must be positive. Based on Z_e and

n_e , the effective permittivity ε_{eff} and permeability μ_{eff} are then calculated as,

$$\varepsilon_{\text{eff}} = n_e Z_e, \quad (\text{S19})$$

$$\mu_{\text{eff}} = \frac{n_e}{Z_e}. \quad (\text{S20})$$

3. Retrieval procedure of acoustic constitutive parameters of an acoustic functional module

For the acoustic case, we also use the scattering matrix, with a_1 , a_2 as the normalized inputs and b_1 , b_2 as the normalized outputs, i.e.,

$$\begin{pmatrix} b_1 \\ b_2 \end{pmatrix} = \begin{pmatrix} S_{11} & S_{12} \\ S_{21} & S_{22} \end{pmatrix} \begin{pmatrix} a_1 \\ a_2 \end{pmatrix}. \quad (\text{S21})$$

The front surface of the metamaterial is located at $z = 0$, and it divides the acoustic system into three regions: the upstream region, the metamaterial region, and the downstream region. An acoustic plane wave $p_{iz} = p_1^+ e^{-jk_{a0}z + j\omega t}$ with amplitude p_1^+ propagates along the z axis through the unit cell of effective thickness d_a . The acoustic wavenumber is $k_{a0} = \omega/c_{a0}$, where c_{a0} is the phase velocity of sound in the air. Omitting the time-harmonic factor $e^{j\omega t}$, the sound pressures and the corresponding particle velocities in the three regions can be written as,

$$p = \begin{cases} p_1^+ e^{-jk_{a0}z} + p_1^- e^{jk_{a0}z} & z < 0 \\ p_2^+ e^{-jk_a z} + p_2^- e^{jk_a z} & 0 \leq z \leq d_a \\ p_3^+ e^{-jk_{a0}(z-d_a)} + p_3^- e^{jk_{a0}(z-d_a)} & z > d_a \end{cases}, \quad (\text{S22})$$

$$v = \begin{cases} \frac{1}{Z_{a0}} (p_1^+ e^{-jk_{a0}z} - p_1^- e^{jk_{a0}z}) & z < 0 \\ \frac{1}{Z_a} (p_2^+ e^{-jk_a z} - p_2^- e^{jk_a z}) & 0 < z < d_a \\ \frac{1}{Z_{a0}} [p_3^+ e^{-jk_{a0}(z-d_a)} - p_3^- e^{jk_{a0}(z-d_a)}] & z > d_a \end{cases}. \quad (\text{S23})$$

Here, the superscripts “+” and “-” denote the forward- and backward-propagating plane waves in the three regions; the acoustic wavenumber $k_a = \omega/c_a$, where c_a is the phase velocity of acoustic waves in the unit cell; $Z_{a0} = \rho_{a0}c_{a0}$ is the characteristic impedance of air, where ρ_{a0} is the air mass density; Z_a denotes the characteristic impedance of the unit cell. If the termination is perfectly anechoic (i.e., $p_3^- = 0$), then S_{11} becomes the ratio of the reflected to the incident pressure ($R = \frac{p_1^-}{p_1^+}$) and S_{21} becomes the ratio of the transmitted to the incident pressure ($T = \frac{p_3^+}{p_1^+}$). Similarly, imposing continuity of both pressure and particle velocity at each boundary leads to explicit formulas for S_{11} and S_{21} .

$$S_{11} = \frac{p_1^-}{p_1^+} = \frac{\left(\frac{Z_a}{Z_{a0}}\right)^2 (1 + W^2) - 1 + 2jW \left(\frac{Z_a}{Z_{a0}}\right)}{\left(\frac{Z_a}{Z_{a0}}\right)^2 (1 + W^2) + 1 + 2j \left(\frac{Z_a}{Z_{a0}}\right) \cot(k_a d_a)}, \quad (S24)$$

$$S_{21} = \frac{2jZ_a Z_{a0} \csc(k_a d_a)}{Z_a^2 (1 + W^2) + Z_{a0}^2 + 2jZ_a Z_{a0} \cot(k_a d_a)}. \quad (S25)$$

W is a dimensionless measure of the strength of Willis coupling. By placing the sound source on the opposite face of the metamaterial, one obtains the remaining scattering parameters S_{12} and S_{22} .

Reciprocity requires $S_{12} = S_{21}$, and S_{22} can then be written as

$$S_{22} = \frac{Z_a^2 (1 + W^2) - Z_{a0}^2 - 2jW Z_a Z_{a0}}{Z_a^2 (1 + W^2) + Z_{a0}^2 + 2jZ_a Z_{a0} \cot(k_a d_a)}. \quad (S26)$$

The acoustic wavenumber k_a and characteristic impedance Z_a are determined by:

$$k_a = \frac{j \ln \zeta + 2\pi m}{d_a}, \quad (S27)$$

$$Z_a = \frac{Z_0 \gamma}{(1 - S_{11})(1 - S_{22}) - S_{12}^2},$$

where

$$\zeta = \frac{1 - S_{11}S_{22} + S_{12}^2 + \gamma}{2S_{12}}, \quad (S28)$$

$$\gamma = \pm \sqrt{(1 - S_{11}S_{22} + S_{12}^2)^2 - 4S_{12}^2}. \quad (S29)$$

Analogous to the electromagnetic case, m denotes the branch index, and the sign of γ is chosen to ensure the real part of Z_a remains positive. The Willis coupling parameter W is defined by

$$W = \pm \frac{S_{22} - S_{11}}{i\gamma}, \quad (S30)$$

and in the quasi-static limit, W is positive.

The effective mass density ρ_{eff} and effective bulk modulus κ_{eff} can be calculated by

$$\rho_{\text{eff}} = \frac{Z_a k_a}{\omega}, \quad (S31)$$

$$\kappa_{\text{eff}} = \frac{Z_a \omega}{k_a}. \quad (S32)$$

4. Numerical models based on the finite element method

In this section, we present the numerical models used for simulations conducted in COMSOL Multiphysics 6.1. The Radio Frequency Module is employed to extract electromagnetic constitutive parameters of the electromagnetic functional module, as illustrated in Fig. S2. The simulation involves exciting an electromagnetic plane wave, denoted by \mathbf{k} , at the incident port. The wave

propagates along the z -axis, with the electric field oriented along the x -axis and the magnetic field oriented along the y -axis. As a result, the magnetic field is perpendicular to the electromagnetic functional module. For the air domains, electric walls are set on the planes perpendicular to the electric field excitation direction, ensuring that the electric field strength \mathbf{E} is zero on these planes. Similarly, magnetic walls are set on the planes perpendicular to the magnetic field excitation direction, where the magnetic field strength \mathbf{H} is zero. To maintain port-matching conditions, perfect matching layers are added outside the incident and output ports.

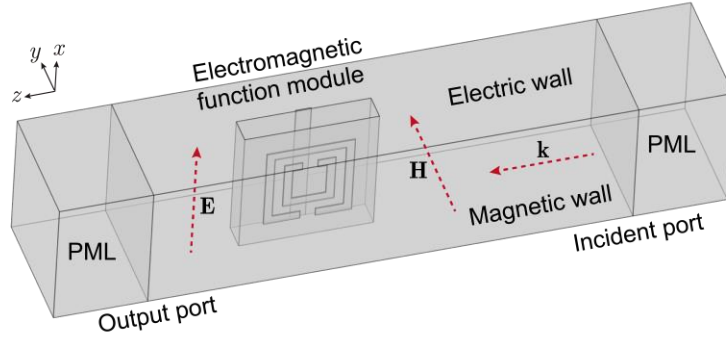


FIG. S2 Schematic of the numerical model for retrieving electromagnetic constitutive parameters

In the numerical model for retrieving acoustic constitutive parameters, the Pressure Acoustic Module is employed to characterize the acoustic functional module and the surrounding air domain. As shown in Fig. S3, a plane-wave background pressure field p_i with an amplitude of 1 Pa is normally incident in the upstream air domain. Upon interacting with the acoustic functional module, a reflected pressure field p_r is generated in the upstream air domain, while a transmitted pressure field p_t propagates in the downstream air domain. Rigid-wall boundary conditions are applied to the four lateral surfaces of the air domains and all edges of the acoustic functional module. Similar to the electromagnetic numerical model, perfect matching layers are incorporated at the inlet of the upstream air domain and the outlet of the downstream air domain to minimize wave reflections.

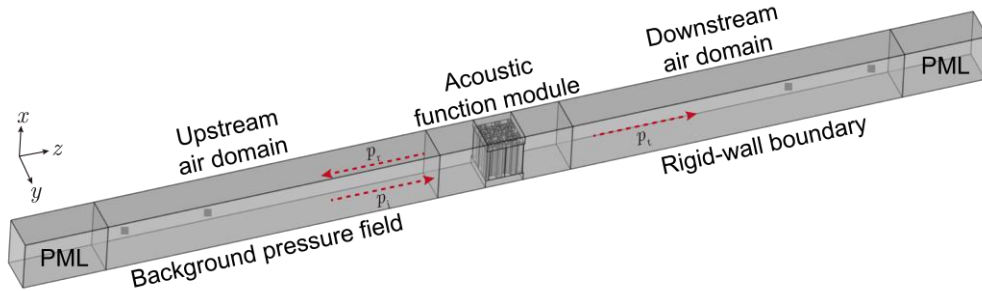


FIG. S3 Schematic of the numerical model for retrieving acoustic constitutive parameters

In the numerical model for evaluating the acoustic beam shift effect, the Pressure Acoustic Module is used to characterize the air domain of the scanning area. As shown in Fig. S4, an internal normal displacement of 2×10^{-6} m is applied at the front end of a waveguide, serving as the sound source. The edges of the sample and waveguide are set as rigid-wall boundaries. Eight perfectly matched layers are implemented to fully enclose the waveguide, sample, and scanning region, providing absorption from all directions.

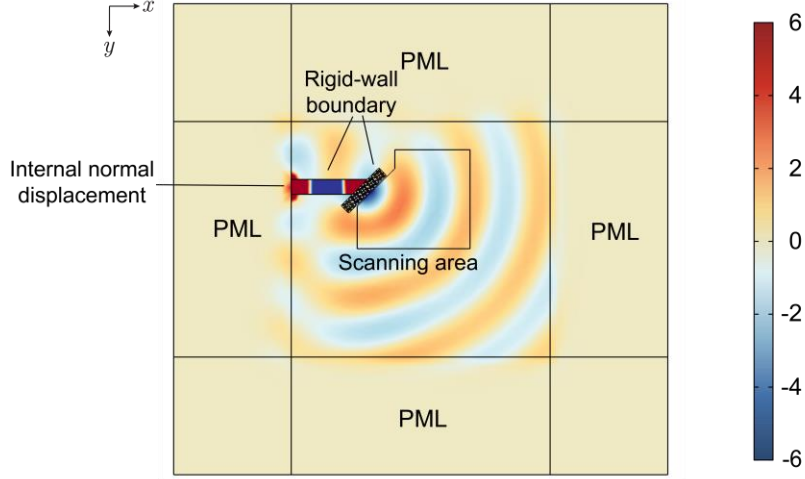


FIG. S4 Schematic of the numerical model for evaluating the acoustic beam shift effect

5. Effective electromagnetic and acoustic refractive indices of the metamaterial

In this section, we present the retrieved effective refractive indices for both electromagnetic and acoustic functional module. The effective electromagnetic refractive index $n_e = \pm\sqrt{\mu_{\text{eff}}\epsilon_{\text{eff}}}$, as shown in Fig. S4 (a), is obtained from the numerically retrieved effective permittivity ϵ_{eff} and permeability μ_{eff} . Similarly, the effective acoustic refractive index $n_a = \pm\sqrt{\rho_{\text{eff}}\kappa_{\text{air}}/(\kappa_{\text{eff}}\rho_{\text{air}})}$, as shown in Fig. S4 (b), is calculated from the retrieved effective mass density ρ_{eff} and bulk modulus κ_{eff} . In these figures, solid lines denote the real parts, and dashed lines denote the imaginary parts. It can be observed that within the dual-negative frequency bands in electromagnetics or acoustics, the effective refractive indices exhibit significantly negative values.

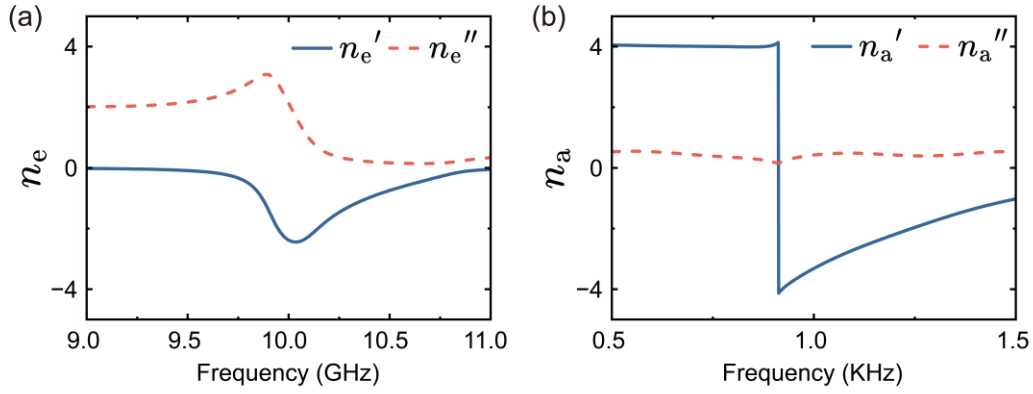


Fig. S5 Retrieved effective refractive indices for electromagnetic and acoustic waves

6. Experimental setup for retrieving acoustic parameters

The effective mass density and bulk modulus of the metamaterial were experimentally characterized using a sound impedance tube. The metamaterial sample was positioned in the downstream section of the tube, which was precisely aligned with the upstream section to ensure continuity. A HiVi M4N loudspeaker, powered by a Weiboer USB-50T amplifier, generated the incident acoustic waves. Four precision microphones (Brüel & Kjær, 4187), designated as M1 through M4, were installed along the tube to capture the resulting pressure fields. The acoustic signals were recorded using a data acquisition device (Brüel & Kjaer Pulse 3560-C).

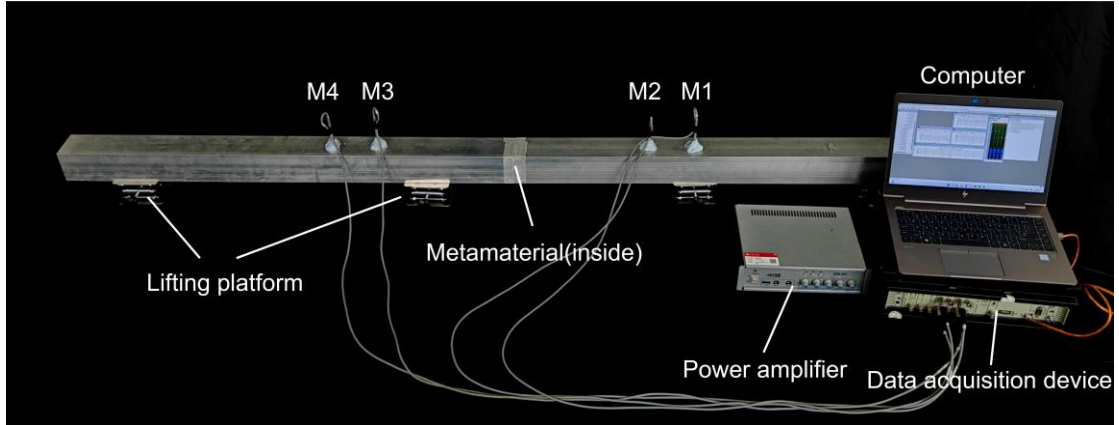


Fig. S6 Experimental setup for retrieving acoustic constitutive parameters

7. Comparison between measured and simulated acoustic constitutive parameters

In order to validate that the PCB walls can be treated as uniform and rigid acoustic boundaries, we retrieved the effective acoustic constitutive parameters of the acoustic functional modules from both simulations and experiments. In the simulations, the PCB walls were modelled as uniform and

rigid acoustic boundaries. Fig. S7 shows the real and imaginary parts of the effective mass density and bulk modulus, normalized to the corresponding values in the air. There are some factors that could contribute to discrepancies between the simulated results and the experimental results. First, there may be a small gap between the sample and the impedance tube, which may lead to changes in the acoustic wave propagation and reflection. Additionally, there may be manufacturing tolerances in the sample, such as slight variations in material dimensions or imperfections. However, despite these potential sources of error, the overall trend and values from the experiments and simulations are in good agreement, supporting the conclusion that the PCB walls can be treated as uniform and rigid acoustic boundaries.

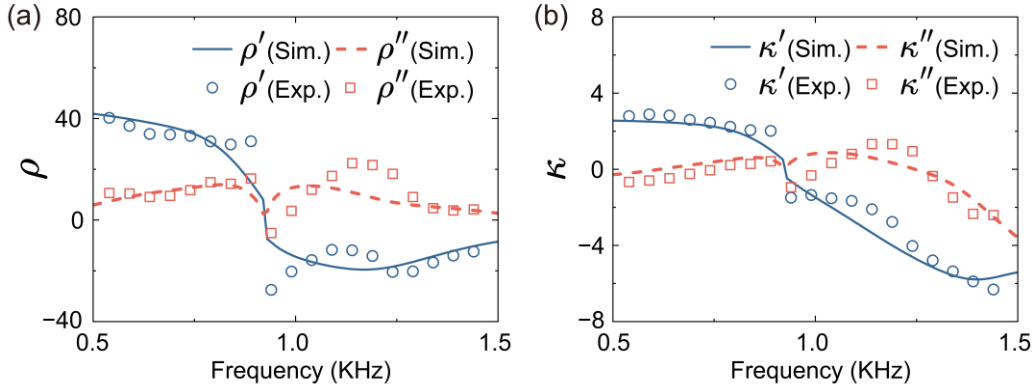


FIG. S7. Comparison of the retrieved acoustic constitutive parameters: numerical simulations vs. experimental measurements

8. Constituent material parameters for the hybrid metamaterial samples

For the hybrid metamaterial samples, the constituent materials comprise polylactic acid (PLA) and PCB (embedded with a thin copper layer). Specifically, PLA is used for 3D-printing the base, lid, and homogeneous walls, with relative permeability of 1 (non-magnetic), relative permittivity of 2.9, electrical conductivity of 5.0×10^{-12} S/m, mass density of 1.24 g/cm^3 , Young's modulus of 3.5 GPa, and Poisson's ratio of 0.36. FR4 is a widely used flame-retardant material in PCBs, with relative permeability of 1 (also non-magnetic), relative permittivity of 4.5, electrical conductivity of 7×10^{-4} S/m, mass density of 1.9 g/cm^3 , Young's modulus of 22 GPa, and Poisson's ratio of 0.15. The concentric split-ring resonators (SRRs) and thin strips within the PCB walls are both composed of 35 μm -thick copper, which has relative permeability of 1, relative permittivity of 4.4, and electrical conductivity of 5.9×10^7 S/m.